

# Freshwater generation from a solar chimney power plant



Tingzhen Ming<sup>a,\*</sup>, Tingrui Gong<sup>b</sup>, Renaud K. de Richter<sup>c,\*</sup>, Wei Liu<sup>b,\*</sup>, Atit Koonsrisuk<sup>d</sup>

<sup>a</sup>School of Civil Engineering and Architecture, Wuhan University of Technology, No. 122, Luoshi Road, Wuhan 430070, China

<sup>b</sup>School of Energy and Power Engineering, Huazhong University of Science and Technology, Wuhan 430074, China

<sup>c</sup>Tour-Solaire.Fr, 8 Impasse des Papillons, F34090 Montpellier, France

<sup>d</sup>School of Mechanical Engineering, Institute of Engineering, Suranaree University of Technology, Muang District, Nakhon Ratchasima 30000, Thailand

## ARTICLE INFO

### Article history:

Received 22 November 2015

Accepted 26 January 2016

Available online 7 February 2016

### Keywords:

Solar chimney

Freshwater

Precipitation

Effectiveness

## ABSTRACT

A modified solar chimney power plant is presented which is not only a solar thermal system able to achieve output power but also is able to extract freshwater from the air. This solar chimney power plant has no greenhouse canopy which is replaced by a collector made of black tubes around the chimney to warm the water and air. The effectiveness of this engineering structure is analyzed in comparison to natural precipitation at nine cities in China; one-dimensional compressible flow and heat transfer mathematical model has been developed to describe the moist air which cools down along the chimney and condenses above the lifting condensation level. The recovery of water is a partial duplication of natural atmospheric convection processes because of the unstable environment lapse rate. The results showed that there is often a high-strength positive correlation between the natural precipitation and the water production by this modified solar chimney power plant in those cities, Water production by the device in the conditions of the study can produce up to  $37.9 \times 10^6$  tons of water per year in Guangzhou, and  $29.7 \times 10^6$  tons of water per year in Chengdu, the correlation coefficient is even up to 0.875. Moreover, this device is more efficient in arid regions, might increase the rainfalls and enhance the regional water cycle. The amount of potable water produced by this modified solar chimney power plant is remarkable and might be able to benefit to several millions of people.

© 2016 Elsevier Ltd. All rights reserved.

## 1. Introduction

### 1.1. Background

Water is an essential item in our lives and promotes civilization. Freshwater shortage is emerging as one of the most critical global resource issues. In China, large areas especially in the North are experiencing a spate of dryness, and even a total national shortage in 2030 is predicted to be nearly 200 billion  $m^3$  with more than 25% for domestic needs [1]. On the other hand, due to global warming and other extreme climatic phenomena, like the El Nino Phenomenon, the droughts are getting more and more serious. The demand for the sustainability of current freshwater is increasing.

To fight global warming, Ming et al. [2] suggested that several types of engineering structures are able to transfer heat from the Earth surface to the upper layers of the troposphere, thus could cool down the Earth by controlling atmospheric convection, enhancing outgoing longwave radiation to the outer space. One of the devices proposed to transfer surface hot air several

kilometers higher, a solar updraft chimney variant was mentioned. A solar chimney power plant (SCPP) usually comprises of three main components: the chimney (for stack effect), the solar collector (the greenhouse, for greenhouse effect) and turbines (power conversion unit, driven by airflow to produce carbon-free electricity). A comprehensive review of scientific literature on SCPP was provided by Zhou et al. [3]. Whereas in the early days Haaf [4] gave some experimental results and a scientific description of the SCPP prototype built in Manzanares, Spain. This experimental plant, with a 194.6 m high chimney and a radius of 5.08 m was built in 1981/82, with a peak output of 50 kW. This prototype was fully tested and validated till 1989.

### 1.2. Literature review

Koonsrisuk [5] compared the performance of the conventional solar chimney power plant and the sloped solar chimney power plant based on second law analysis. Meanwhile, a single dimensionless similarity variable for the solar chimney power plant was proposed by Koonsrisuk and Chitsomboon [6]. Kraetzig [7] described and formulated the thermo-fluid dynamics including all physical processes in the SCPPs to evaluate the energy harvest by them. Bernardes and Backström [8] studied the performance

\* Corresponding authors.

E-mail addresses: [tzming@whut.edu.cn](mailto:tzming@whut.edu.cn) (T. Ming), [renaud.derichter@gmail.com](mailto:renaud.derichter@gmail.com) (R.K. de Richter), [w\\_liu@hust.edu.cn](mailto:w_liu@hust.edu.cn) (W. Liu).

## Nomenclature

|                   |   |                      |   |
|-------------------|---|----------------------|---|
| $A$               | chimney cross-section area ( $\text{m}^2$ )                             | $V_0$                | velocity at the inlet (m/s)                                       |
| $c_p$             | specific heat capacity ( $\text{J}/(\text{K kg})$ )                     | $V_i$                | condensed water velocity (m/s)                                    |
| $d$               | chimney diameter (m)  | $Z$                  | vertical height (m)   |
| $d_s$             | moisture content in per kilogram air ( $\text{kg}/\text{kg}$ (dry air)) | $C$                  | atmospheric scale height (m)                                      |
| $f$               | friction factor   | $R_g$                | ideal gas constant ( $\text{J}/(\text{kg K})$ )                   |
| $g$               | gravitational acceleration, $9.8 \text{ (ms}^{-2}\text{)}$              | <i>Greek symbols</i> |   |
| $H$               | chimney height (m)  | $\Delta$             | difference  |
| $L$               | latent heat ( $\text{J}/\text{kg}$ )                                    | $\kappa$             | specific heat ratio   |
| $\dot{m}$         | condensed water in per kilogram air ( $\text{kg}/\text{kg}$ )           | $\rho$               | density ( $\text{kg}/\text{m}^3$ )                                |
| $\dot{m}_{total}$ | mass flow rate ( $\text{m}^3/\text{s}$ )                                | $\rho_H$             | air density at the exit of the chimney ( $\text{kg}/\text{m}^3$ ) |
| $p$               | pressure (Pa)   | $\varepsilon$        | the entrance and exit losses factor                               |
| $p_v$             | water vapor partial pressure (Pa)                                       | <i>Subscripts</i>    |   |
| $p_s$             | saturated water vapor partial pressure (Pa)                             | $0$                  | chimney inlet   |
| $p_z$             | pressure at some height (Pa)  | $H$                  | chimney outlet  |
| $s$               | water content in per cubic meter ( $\text{kg}/\text{m}^3$ )             | $l$                  | water liquid  |
| $t$               | Celsius temperature ( $^\circ\text{C}$ )                                | $s$                  | saturated state   |
| $T_0$             | heated air temperature at the chimney entrance (K)                      | $v$                  | water vapor   |
| $T_z$             | temperature at some height (K)  |                      |   |
| $v$               | specific volume ( $\text{m}^3/\text{kg}$ )                              |                      |   |
| $V_z$             | vertical velocity (m/s)   |                      |   |

for the heat transfer coefficients of Pretorius and Kroger [9] by theoretical simulations, each subjected to two power control schemes. Fasel et al. [10] simulated the performance of SCPP by using ANSYS Fluent and an in-house developed Computational Fluid Dynamics (CFD) code. To decrease the negative influence of ambient cross-wind on the SCPPs performance, Ming et al. [11] simulated a blockage wall built a few meters in front of the collector inlet by numerical simulation. Ferreira et al. [12] studied the feasibility of a solar chimney for food drying. Maia et al. [13] performed an analytical and numerical study of the influence of geometric dimensions and materials on the flow behavior in a solar chimney, the energy and exergy analyses were also carried out [14]. Patel et al. [15] studied the effects of various geometric parameters on a SCPP to evaluate its performance. Cao et al. [16] studied a sloped solar SCPP in Lanzhou, which presented technical and practical support for SCPP. Ninic and Nizetic [17] studied the possibility of developing and making use of the availability of warm, humid air in the atmosphere. Nizetic et al. [18] analyzed the feasibility of SCPPs as an environmentally acceptable energy source for small settlements and islands in the Mediterranean region. Nizetic and Klarin [19] evaluated the factor of turbine pressure drop in SCPP by a simplified analytical approach. Pasumarthi and Sherif [20] studied the performance characteristics of solar chimneys both theoretically and experimentally by a demonstration model, the overall results were encouraging [20].

Since Schlaich et al. [21] introduced the SCPPs, with a good overview of the technology, many researchers have been trying to find conceptual devices which operate in a more effective fashion. Zou et al. [22] proposed the hybrid cooling-tower-solar-chimney system, which could generate electricity and dissipate waste heat simultaneously. A device called Solar Cyclone was introduced for accomplishing the separation of water from surface air by Kashiwa and Kashiwa [23]. There is an expansion cyclone separator for condensing and removing atmospheric water in the chimney, with the central temperature below the dew point. If it works, the fresh water can be collected and this cycle is sustainable, but the efficiency is unclear, and should be determined in further studies.

The construction cost of an SCPP could be approximately broken down as follows: 25% for the chimney, 5% for the turbines and 70% for the collector [24]. Thus for cutting down expenses, Bonnelle [25] proposed a variant SCPP with no collector, similar to the "energy tower" also described by Bonnelle.

In addition, Papageorgiou [26] studied solar chimney technology without solar collector with floating chimney. As the solar collector received thermal energy by the sunlight irradiation to create warm air, it is evident that the heat is necessary for solar chimney operation, but these researchers found that the air humidity and condensation in the chimney can increase the updraft velocity, thanks to the latent heat released inside the chimney, thus the solar collectors could be omitted. In addition, they suggested that the solar chimney power plant placed in humid areas, near the sea, could generate more power output than that placed in arid areas.

Zhou et al. [27] investigated a combined solar chimney system for power generation and seawater desalination. One-dimensional compressible flow model was developed to compare the performance of the classical SCPP system and the combined solar chimney system for power generation and seawater desalination. They found that due to the fact that an important amount of heat is used as latent heat for water evaporation, decreasing the working air temperature, the power output of the combined system is less than that of the classical system. Moreover, a revenue analysis carried out found that the critical chimney height depends on the price level of fresh water and of electric power.

### 1.3. Research in this article

In this paper, a modified solar chimney power plant with no greenhouse canopy was proposed; the collector being replaced by twisted black tubes filled with hot water to warm the air entering the chimney and to keep the relative humidity percent identical to ambient. Then, a one-dimensional compressible flow and heat transfer mathematical model was developed to investigate the effectiveness of freshwater generation by this unique engineering structure. Later, the natural precipitations at nine cities in China were compared to effectiveness of freshwater generation by this unique engineering structure.

## 2. System mechanism and prototype

### 2.1. System mechanism

Starr and Anati [28] proposed an artificial construction within a vertical tube of 3 km height with a radius of 50 m, which they

named aerological accelerator (AeAc). It works on the principle that there is potential energy in the atmosphere. As an air parcel rises, the temperature decreases, which causes the relative humidity to increase. When the air reaches the lifting condensation level where the air temperature drops under the dew point inside the tube, water vapor will begin to condense onto any available solid surfaces: this is the same process by which clouds form. Fresh water would be produced. The recovery of water is a partial duplication of natural atmospheric convection processes because of the unstable environment lapse rate, which will produce turbulence in the atmosphere [29]. Fig. 1 shows the similar device, hot and humid air flow is induced through a warm seawater shower.

2.2. Prototype

There were actual prototypes for the AeAc in existence and described by Carte [30] and Lambrechts [31]. These models used a ventilation shaft through which air leaves a deep hole mine. At the Joint Ventilation Shaft situated inside the property of Springs Mines in Johannesburg for the year of 1948, field measurements showed that the air flow was higher than 28 316 cubic meters per minute on some days, while normally the quantity was between 21 237 and 22 653 cubic meters per minute. It was verified that the shaft bottom was almost dry when the air quantity was over 28 316 cubic meters per minute, but a downpour of water occurred at the bottom of the shaft when the air flow was 22 653 cubic meters per minute or less. Furthermore, when the ventilation fan was stopped, no water was found and it was concluded that the water was all condensed from the air. Lambrechts indicated that this mine shaft was one of the world’s successful artificial rain-makers [31].

There is a proposal to extract more humidity from the air in mine shaft using a moisture-absorbing solution, such as CaCl<sub>2</sub> or LiBr. When moist air passes over the surface of the absorbent, water vapor is absorbed. The latent heat of vaporization released during absorption process heats the air. Consequently, the air in the right passage (3–4) in Fig. 2 is less dense than that in the left passage (1–2). So the air rises in the right passage while it sinks in the left passage. In addition, the diluted absorbing solution could be re-concentrated with solar evaporators, thus the system can operate continuously. The air compression is accomplished by the hydrostatic pressure change as the air flows down in the left passage, while the air expansion occurred in the right passage.

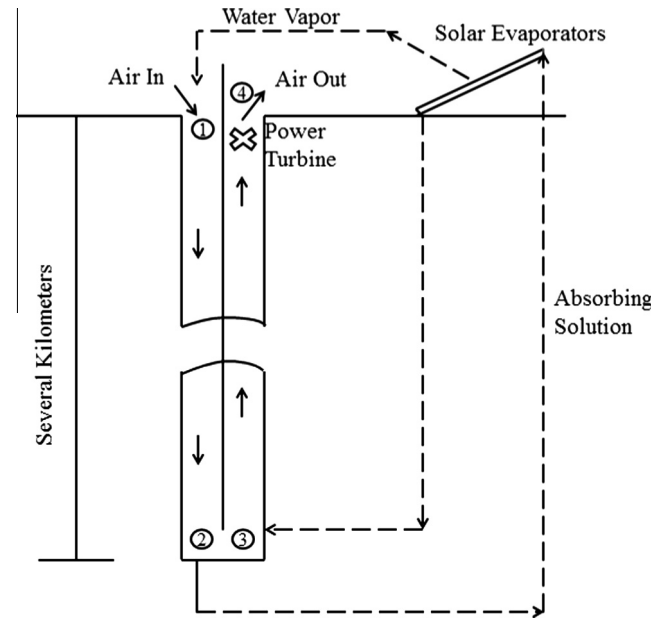


Fig. 2. Ventilation shaft for very deep mines.

Work is extracted via the turbine installed at the top opening of the hole. Basically, the cycle explained is similar to the cycle of SCPP to some extent.

Unlike the AeAc, the mine shaft has a small radius to depth ratio, due to the proportionally large area of the shaft wall, the friction losses are more important, but can be minimized by keeping air velocity low. Meanwhile, there is a turbine (fan) used to create the updraft and overcome this friction.

Starr and Anati [32] studied the effectiveness of AeAc at five different locations. They examined whether a period of low precipitation is favorable or unfavorable for water production by the AeAc. They computed the ratio of the AeAc production to natural precipitation and deduced that the ratio in arid regions is higher than that in rainy regions.

3. Model description

3.1. Physical model

As a matter of fact, the device proposed in this article is similar to chimney or smokestack: a hot and humid air flow is induced through a warm water shower at the bottom of the tower. Because of the air density difference between the inside and outside, the air flow is guided upward by convection. As the chimney is high enough, adiabatically ascending air within the chimney should reach the lifting condensation level, where precipitation will occur releasing latent heat inside the conduit tower, warming the air, which is able to rise more.

As shown in Fig. 3, the SCPP variant of this article has black tubes instead of a collector, so the installation cost is less expensive. In fact, these black tubes not only act as a solar collector, but also store thermal energy. The water filled inside the black tubes is exposed to the sun and heated by absorbing sunlight radiation. At night, when the air starts to cool down, the water inside the tubes releases the heat stored during the day. In addition, the thermal storage with water works more efficiently due to the fact that the heat capacity of water per kg is higher than the heat capacity of air, sand or gravel.

In this paper, the SCPP variant device configuration considered is as in Fig. 3. The best choice of selecting a site might be the

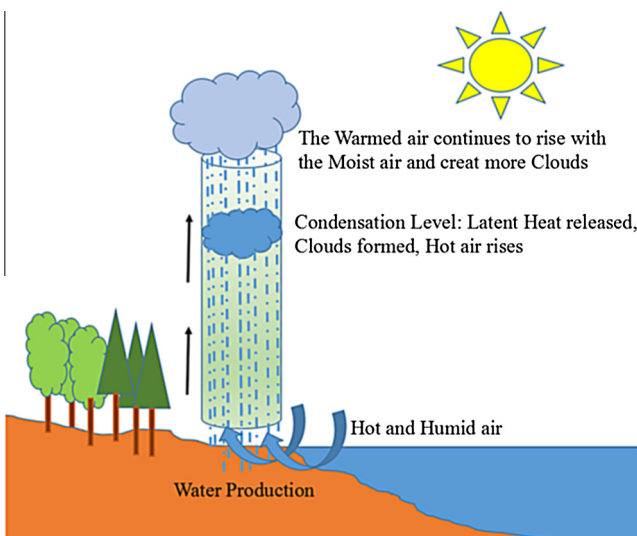


Fig. 1. The process of a SCPP with water vapor condensation.

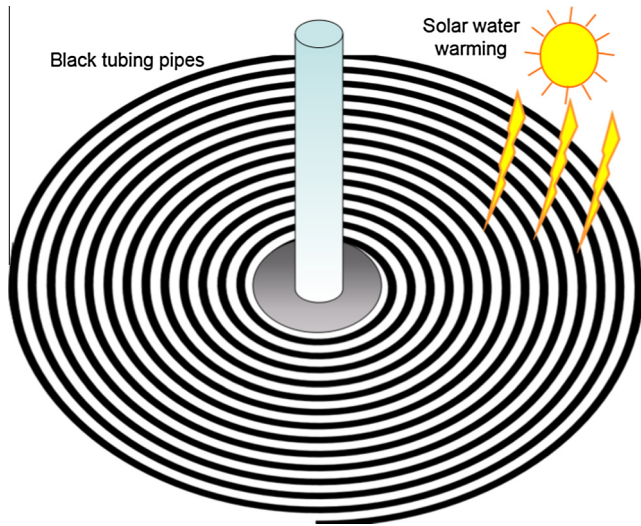


Fig. 3. SCPP variant system with a coil of black tube working as the solar collector.

seaside, because of such factors as the prevailing wind region, humidity, insolation and environmental lapse rate. But the coastal condition seems a little harsh, so we use water-filled black tubes to warm the air at a higher temperature than ambient air in other inland cities to study the effectiveness of this device. The radius of the chimney studied is 50 m, and for the purpose of studying the effectiveness of this device, we assumed that the circular cylinder chimney is 3000 m height as done by Starr and Anati [28].

Compared with the traditional SCPP, two technical issues should be pointed. (a) Less tubing maintenance than glass on usual SCPP collector can be achieved. The effect of sand blown by the wind on the glass canopy is deleterious; it becomes easier to clean up tubing pipes than glass, or than a flat polycarbonate collector (Fig. 3). (b) No turbines are installed in this model as the present system which is dedicated to produce water; much less moving mechanical systems are used but we need some electrical input to drive pumps inside the tubing. If we install turbines in the system to meet the required electrical input of running the water tubing pipes, the maintenance fee will be less than that of the traditional SCPP.

### 3.2. Mathematical model

The performance of the SCPP greatly depends on the chimney dimensions, initialization conditions and ambient conditions.

There are some assumptions made in this model to simplify the calculations as follows:

- The pressure within the chimney at the chimney top  $P_H$  is the same as in the adjacent environment at the same altitude;
- The radius of the chimney is large enough, so that the parameters change only along the altitude;
- The environmental conditions are steady;
- The chimney is a circular cylinder;
- The wall of the chimney is thermally insulated;
- No super saturation occurs; water droplets once formed, precipitate on the chimney walls and do not induce airflow perturbation.
- The temperature of the black tubes is assumed to be higher enough to warm the air entering the tower to 5 K higher than that of the ambient, and hot water showers keep the same relative humidity of the intake air at the entrance of the chimney with that of the ambient air.

The conditions of the environment are changing all over the time. The variations, such as the atmospheric temperature, pressure, relative humidity (RH), are changing with location and time. Here we employed the standard atmosphere as the working condition. By using water-filled black tubes to absorb diffuse radiation and work as a heat storage system, the chimney is able to operate 24 h on pure solar energy, it is crucial for those regions with abundant solar radiation. Accordingly, we assumed that the chimney operates  $365 \times 24$  h, it means the operating time is 100%, and the water collecting mechanism inside the chimney is supposed to be 100% efficient (see Fig. 4).

The pressure, temperature, and density variation of the air outside the chimney can be calculated by [33]:

$$T_{\infty}(z) = T_{\infty}(0) \left( 1 - \frac{\kappa - 1}{\kappa} \frac{z}{C} \right) \quad (1)$$

$$p_{\infty}(z) = p_{\infty}(0) \left( 1 - \frac{\kappa - 1}{\kappa} \frac{z}{C} \right)^{\kappa/(\kappa-1)} \quad (2)$$

$$\rho_{\infty}(z) = \rho_{\infty}(0) \left( 1 - \frac{\kappa - 1}{\kappa} \frac{z}{C} \right)^{1/(\kappa-1)} \quad (3)$$

For planetary atmosphere, atmospheric scale height is the increase in altitude for which the atmospheric pressure decreases. The atmospheric scale height remains constant for a particular temperature. It can be calculated by:

$$C = \frac{R_g T_{\infty}(0)}{g} \quad (4)$$

and  $\kappa = 1.235$  (standard atmosphere), where  $T_{\infty}$  is the ambient temperature;  $p_{\infty}$  is the ambient air pressure;  $\rho_{\infty}$  is the ambient

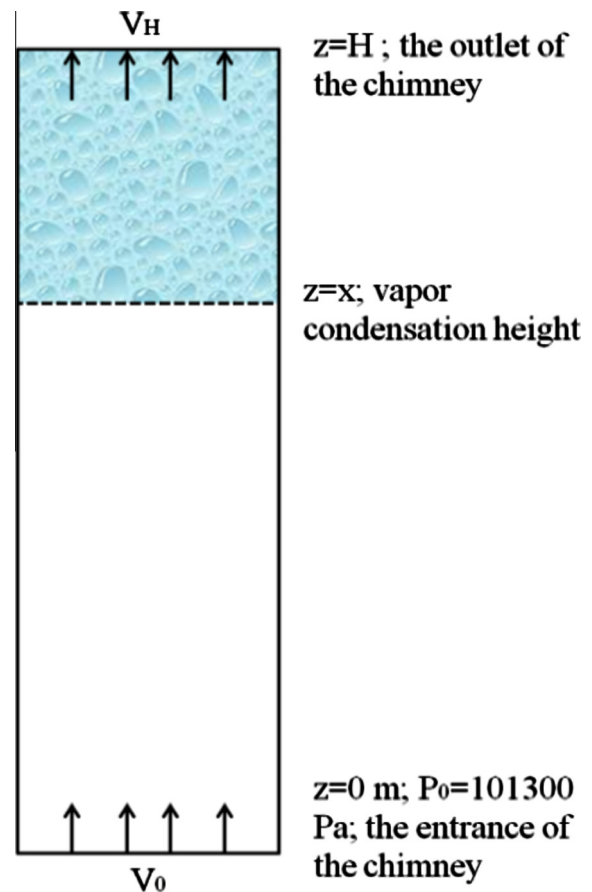


Fig. 4. The geometry of the chimney.

air density;  $z$  represents the height above ground level;  $R_g$  is the ideal gas constant, which is 287.05 J/(kg K);  $g$  is the gravitational acceleration, which is 9.8 m/s<sup>2</sup>;  $\kappa$  is the specific heat ratio.

The driving potential, the buoyancy force, inside the chimney can be expressed by the integral:

$$\Delta p = g \int_0^H (\rho_\infty(z) - \rho(z)) dz \quad (5)$$

where  $H$  is chimney height;  $\rho_\infty(z)$  and  $\rho(z)$  are ambient air density and internal airflow density inside the chimney at any height  $z$ , respectively.

The energy conservation equation can be written as:

$$C_p(T_0 - T_z) + \dot{m}L = gz + \frac{1}{2}(1 - \dot{m})V_z^2 + \frac{1}{2}\dot{m}V_l^2 - \frac{1}{2}V_0^2 \quad (6)$$

where  $C_p$  is the air specific heat capacity, here we take as 1005 J/(kg K);  $T_z$  and  $V_z$  are air temperature and velocity at height  $z$ ;  $V_l$  is the liquid velocity relative to air flow. The difference among  $V_z$  and  $V_0$  is quite small because the shape of the chimney is cylindrical (the equation reminds us that a nozzle shape design at the top of the chimney will be effective to reduce the air flow temperature, helping to form clouds or precipitation), and  $\dot{m}$  is relative small, so we can rewrite Eq. (6) as:

$$T_z = T_0 - \frac{(gz - \dot{m}L)}{C_p} \quad (7)$$

In general, the total pressure of moist air is atmospheric pressure which is comparatively low, so the partial pressure of dry air and water vapor are lower, and the moist air can be regarded as an ideal gas mixture. The ideal gas state equation is:

$$p v = R_g T \quad (8)$$

The temperature difference in the system is small (less than 50 K in most cases), so the latent heat for vapor condensation can be seen as a constant value ( $L = 2257000$  J/kg). Since the vapor partial pressure is rather small when compared to the total moist air pressure,  $R_g$  can be assumed to be constant in the calculations.

The partial pressure of water vapor is a function of the temperature  $t$  expressed in °C and it can be calculated by the Arden Buck approximate equation:

$$p_s = 611.21 \cdot \exp\left(\frac{(18.678 - t/234.5) \cdot t}{257.14 + t}\right) \quad \text{for } -80^\circ\text{C} < t < 50^\circ\text{C} \quad (9)$$

The RH for the air is defined as

$$\text{RH} = \frac{p_v}{p_s} \quad (10)$$

where  $p_s$  represents the partial pressure for the saturated moist air.

The water content per kilogram of dry air is

$$d_s = 0.622 \cdot \frac{p_v}{p_z - p_v} \quad (11)$$

The water content per kilogram of moist air is

$$s = 0.622 \cdot \frac{p_v}{p_z - 0.378p_v} \quad (12)$$

Assuming a linear variation of air density with height, the density in the chimney can be described as

$$\rho(h) = \rho_0 - (\rho_0 - \rho_H) \cdot \frac{z}{H} \quad (13)$$

The updraft potential can be partly undermined by the wall friction, and other points losses along the chimney, the momentum conservation equation for the flow in the direction of chimney axis is given by Kashiwa and Kashiwa [23]

$$\Delta p(1 - n) = \left[ \varepsilon + e^{H/C} + \frac{f \cdot C}{d} \right] \cdot \frac{1}{2} \rho_0 V_0^2 \quad (14)$$

where  $n$  is factor of pressure drop at the turbine (when not considering the power output, the factor can be set equal to 0;  $V_0$  is the flow velocity in the chimney axial direction at the inlet of the chimney. Coefficients in the brackets represent the exit loss (with unit coefficient), other point losses, and wall friction. The factor  $\varepsilon$  accounts for the following energy losses: (1) the energy losses in the turbine; (2) energy losses at the location where the flow area changes; (3) the turbulent flow losses; (4) the vapor condensation at any location of the chimney. The wall is not too rough, so  $f = 0.01$  for high Reynolds number flow in a pipe is adopted in the calculation.

The total moist air mass flow in the chimney is

$$m_f = \rho_0 V_0 A = \rho_H V_H A + m_f \cdot s \quad (15)$$

where  $\rho_0$  and  $A$  are the moist air density and cross-sectional area of the chimney,  $m_f$  is the total mass flow through the chimney.

The iteration is listed in the following chart as shown in Fig. 5.

To test the validity of the mathematical model, the calculated results are compared to the experimental data collected from the SCPP operated in Manzanares, Spain [4]. When there is no turbine load ( $\varepsilon = 0.1$ ,  $f = 0.01$ ,  $n = 0$ ), the calculated updraft velocity at the entrance of the chimney is 12.22 m/s, the difference is 0.75%. When the turbine load factor is set  $n = 0.67$ , the calculated updraft velocity at the entrance of the chimney is 7.02 m/s, the difference is 6.4%. As Table 1 shows, both cases seem to meet well with the experimental data. The disparity between them could be attributed to reasons such as different selection of heat transfer coefficients, flow resistance model and ignoring the influence of ambient relative humidity which was not taken into consideration in the experimental Spanish plant. Besides, the mathematical model in this paper includes the compressible nature of the atmosphere, and these experimental results were obtained only with a very short chimney. When the chimney is high enough to a height above the lifting condensation level where condensation occurs, the calculated results could be affected. To solve this, we compared with parameters from [34] in different ambient relative humidity as follows:  $h = 1500$  m;  $d = 160$  m;  $(\Delta T/T_0) = (20/303.2)$ ;  $f = 0.008428$ ;  $\varepsilon = 0.5$ . The calculated results give the difference of updraft velocity within 10%. To conclude, the mathematical model proposed in this paper is effective and feasible as it is comparable to the reference.

## 4. Results and discussion

### 4.1. Comparisons

The results obtained by a hypothetical SCPP of 50 m radius extending vertically to 3000 m at the nine stations in China are shown in Fig. 6 by monthly average value in comparison with the natural precipitation at the respective locations. The initial conditions used in the calculation for different cases include the monthly average ambient temperature and the monthly average ambient humidity of the nine stations, as shown in Tables 2 and 3. The source of the meteorological data used in this paper for the calendar year 2013 is the National Bureau of Statistics of the People's Republic of China [http://www.stats.gov.cn/] (see Table 4).

Fig. 6(a) represents the situation in Chengdu. It is clear that the main portion of precipitation occurs in summer months, from June to September. On the one hand, there is a strong peak in July, which reaches up to 525.5 mm, what's more, the precipitation which just less than the maximum is only 228.3 mm, thus the variation during summer months is important. Conversely, the precipitation of other months changes comparatively slightly, in fact, there is little rainfall during the other months. On the other hand,

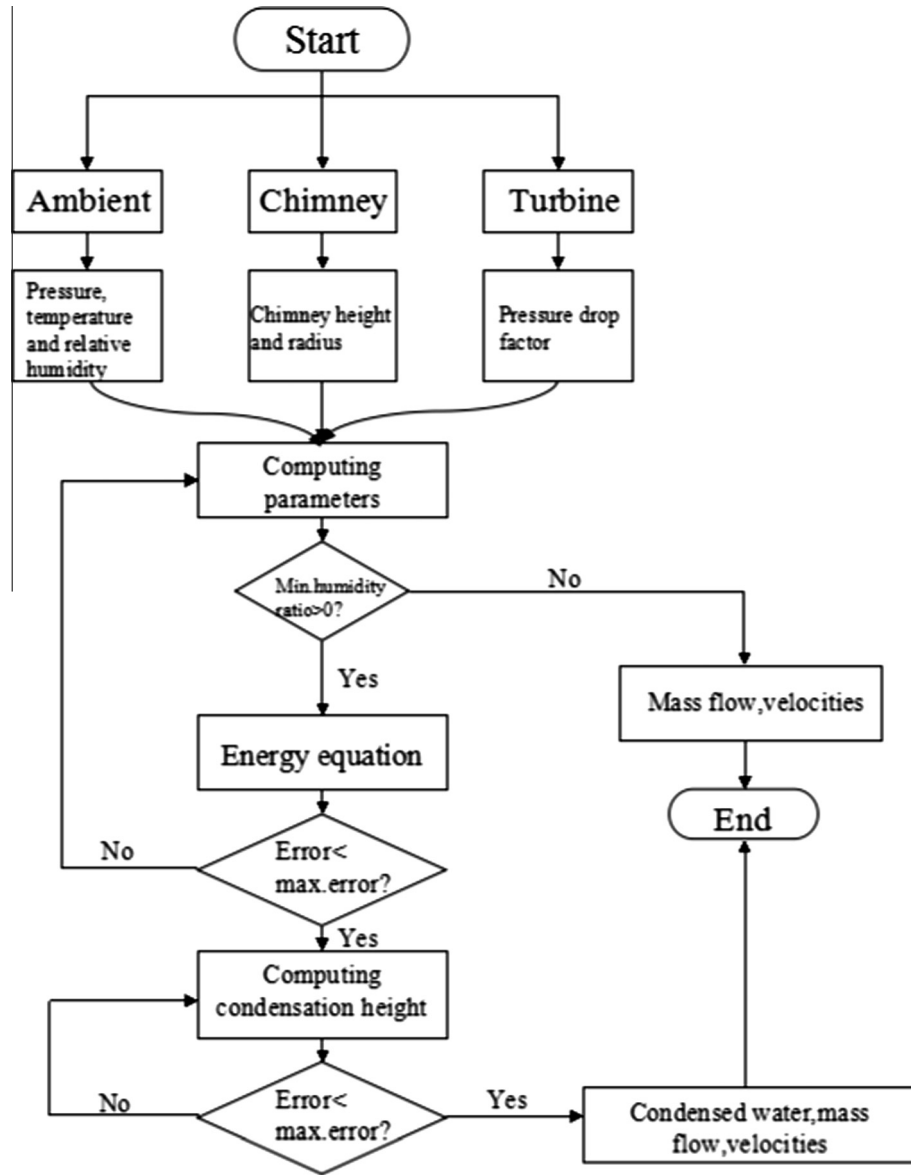


Fig. 5. The iteration flow chart for the mathematical model.

**Table 1**  
Comparisons between computed results of updraft velocity at the entrance of the chimney and experimental results of Manzanares, Spain.

| Case  | Case 1<br>( $\varepsilon = 0.1$ ,<br>$f = 0.01$ ,<br>$n = 0$ ) | Experimental<br>data 1<br>( $\varepsilon = 0.1$ ,<br>$f = 0.01$ , $n = 0$ ) | Case 2<br>( $\varepsilon = 0.1$ ,<br>$f = 0.01$ ,<br>$n = 0.67$ ) | Experimental<br>data 2 ( $\varepsilon = 0.1$ ,<br>$f = 0.01$ ,<br>$n = 0.67$ ) |
|---|--|---|---|--|
| Updraft velocity at the entrance of the chimney (m/s) | 12.2   | 12  | 7.0   | 7.5  |
| Difference  | 1.8%   |   | 6.4%  |  |

the sharp maximum in SCPP output coincides exactly with the maximum in natural precipitation observed in July. In addition, the two curves variation tendencies are similar; the only difference between them is that the SCPP variant output curve is smoother. There seems to be some positive correlation between the SCPP results and natural precipitation.

Here we defined that a positive correlation is when the two curves follow the same tendency: increasing or decreasing at the same time, maximums and minimums at the same time during the same months. Fig. 6(b) represents the situation in Shanghai. The variation tendencies of the two curves are almost similar during the first eight months. From August to December, the seasonal variation is maximal between two curves; it shows that the precipitation curve changes greatly. There is a strong peak up to 291.7 mm during the month of October in natural precipitation, and a sharp minimum of precipitation of only 20.4 mm in November. It can be concluded that there still exists some positive correlation between the water production of this SCPP variant device and natural precipitation.

Fig. 6(c) and (d) shows the natural precipitation and water production by the SCPP variant device of Shijiazhuang and Zhengzhou, respectively. The total precipitation in Shijiazhuang for the calendar year 2013 is 508.3 mm, and in Zhengzhou is only 353.2 mm, obviously these two are comparatively arid regions.

In the case of Shijiazhuang there seems to be a positive correlation between the two curves, it shows that the SCPP variant output

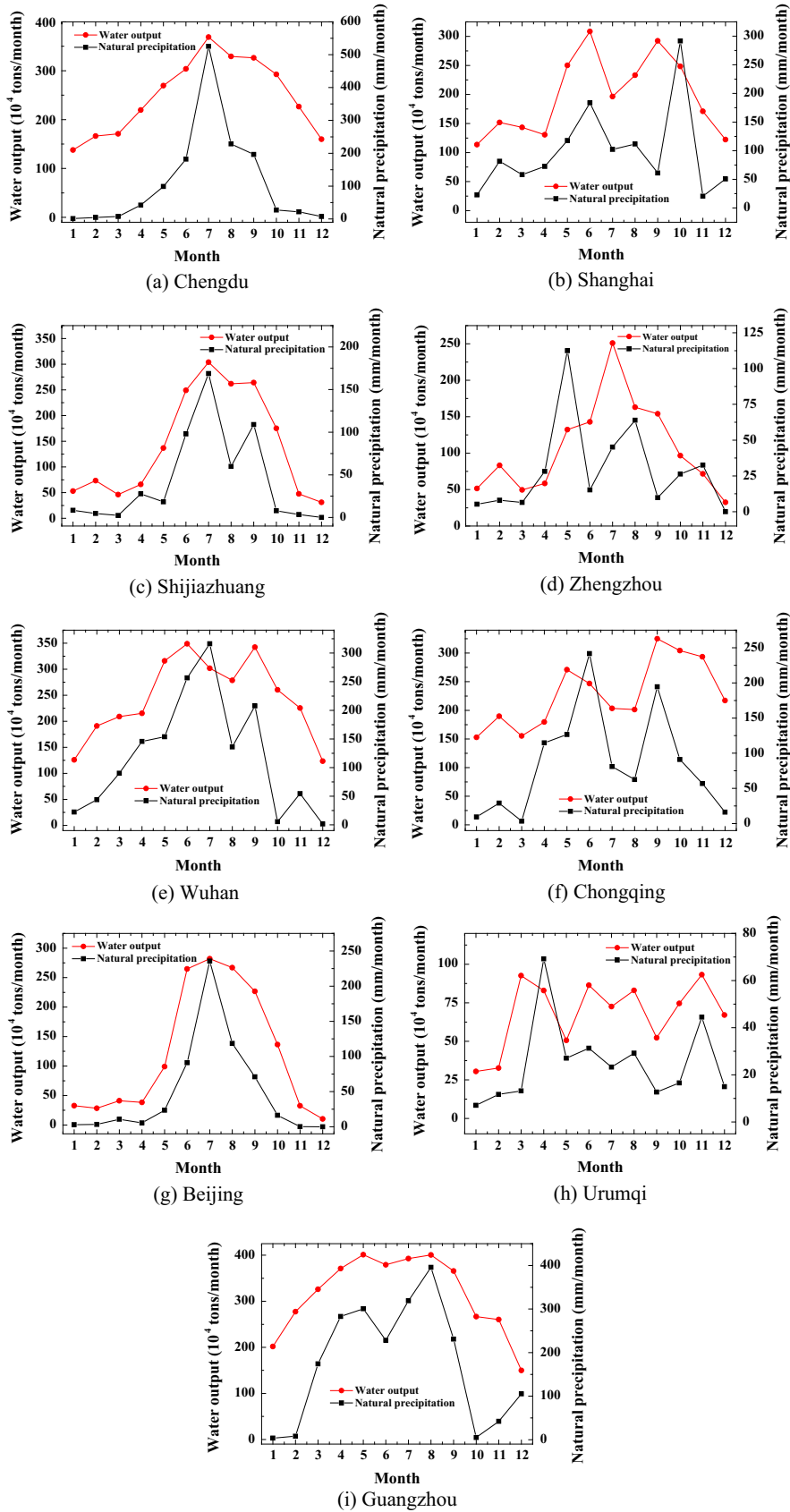


**Fig. 6.** In black the natural precipitation (NP) in millimeters per month versus in red the SSCP water output in  $10^4$  tons per month are shown for the calendar year 2013 at (a) Chengdu, (b) Shanghai, (c) Shijiazhuang, (d) Zhengzhou, (e) Wuhan, (f) Chongqing, (g) Beijing, (h) Urumqi, (i) Guangzhou. (For interpretation of the references to color in this figure legend, the reader is referred to the web version of this article.)

**Table 2**  
Monthly average ambient temperature in °C of the nine stations used in the calculation.

| Cities       | Jan. (°) | Feb. (°) | Mar. (°) | Apr. (°) | May (°) | Jun. (°) | Jul. (°) | Aug. (°) | Sep. (°) | Oct. (°) | Nov. (°) | Dec. (°) |
|--------------|----------|----------|----------|----------|---------|----------|----------|----------|----------|----------|----------|----------|
| Chengdu      | 5.3      | 9.3      | 15.7     | 17.7     | 21.2    | 24.5     | 25.8     | 26.5     | 20.8     | 17.6     | 12.0     | 6.0      |
| Shanghai     | 4.6      | 6.8      | 11.0     | 15.3     | 21.3    | 24.1     | 32.0     | 31.0     | 25.0     | 20.0     | 13.4     | 6.1      |
| Shijiazhuang | −4.2     | −0.4     | 8.7      | 13.8     | 22.2    | 24.9     | 27.3     | 27.9     | 21.4     | 14.7     | 8.1      | 1.7      |
| Zhengzhou    | −0.5     | 3.1      | 11.0     | 16.0     | 22.8    | 27.0     | 29.1     | 30.1     | 23.5     | 17.2     | 9.7      | 3.6      |
| Wuhan        | 2.9      | 5.9      | 12.9     | 17.1     | 22.1    | 26.1     | 30.6     | 30.6     | 22.9     | 18.2     | 11.4     | 4.5      |
| Chongqing    | 8.3      | 11.9     | 17.9     | 20.3     | 22.5    | 27.9     | 31.5     | 30.5     | 23.4     | 19.7     | 14.7     | 9.3      |
| Beijing      | −4.7     | −1.4     | 6.2      | 12.6     | 21.9    | 23.8     | 27.4     | 27.3     | 20.7     | 13.6     | 6.3      | 0.1      |
| Urumqi       | −10.3    | −10.1    | 5.5      | 12.4     | 16.6    | 21.5     | 23.6     | 22.8     | 17.5     | 11.4     | 0.2      | −6.8     |
| Guangzhou    | 13.3     | 17.3     | 19.2     | 20.6     | 25.3    | 27.6     | 27.4     | 27.5     | 26.5     | 22.9     | 19.0     | 11.9     |

**Table 3**  
Monthly average ambient humidity in RH% of the nine stations used in the calculation.

| Cities       | Jan. (%) | Feb. (%) | Mar. (%) | Apr. (%) | May (%) | Jun. (%) | Jul. (%) | Aug. (%) | Sep. (%) | Oct. (%) | Nov. (%) | Dec. (%) |
|--------------|----------|----------|----------|----------|---------|----------|----------|----------|----------|----------|----------|----------|
| Chengdu      | 75       | 73       | 64       | 70       | 74      | 76       | 84       | 78       | 83       | 82       | 80       | 79       |
| Shanghai     | 70       | 75       | 65       | 57       | 71      | 77       | 58       | 63       | 74       | 72       | 67       | 69       |
| Shijiazhuang | 71       | 69       | 44       | 45       | 53      | 68       | 74       | 68       | 73       | 66       | 45       | 47       |
| Zhengzhou    | 60       | 64       | 43       | 42       | 52      | 52       | 66       | 54       | 55       | 49       | 50       | 45       |
| Wuhan        | 78       | 87       | 75       | 70       | 80      | 81       | 72       | 69       | 83       | 76       | 81       | 73       |
| Chongqing    | 72       | 73       | 59       | 61       | 73      | 66       | 59       | 59       | 80       | 81       | 87       | 84       |
| Beijing      | 61       | 51       | 45       | 39       | 47      | 71       | 71       | 69       | 68       | 60       | 42       | 40       |
| Urumqi       | 79       | 80       | 62       | 50       | 40      | 45       | 42       | 44       | 40       | 49       | 75       | 89       |
| Guangzhou    | 73       | 80       | 85       | 90       | 89      | 84       | 86       | 87       | 83       | 72       | 75       | 65       |

**Table 4**  
Monthly average natural precipitation in mm of the nine stations used in the calculation.

| Cities       | Jan. | Feb. | Mar.  | Apr.  | May   | Jun.  | Jul.  | Aug.  | Sep.  | Oct.  | Nov. | Dec.  |
|--------------|------|------|-------|-------|-------|-------|-------|-------|-------|-------|------|-------|
| Chengdu      | 1.2  | 4.7  | 7.6   | 42.2  | 99.0  | 182.1 | 525.5 | 228.3 | 196.2 | 27.1  | 21.8 | 7.6   |
| Shanghai     | 22.8 | 81.5 | 58.1  | 72.5  | 117.7 | 183.5 | 102.1 | 111.5 | 61.1  | 291.7 | 20.4 | 50.5  |
| Shijiazhuang | 8.4  | 4.7  | 2.4   | 27.7  | 18.3  | 97.9  | 168.7 | 59.9  | 108.9 | 7.9   | 3.5  | 0     |
| Zhengzhou    | 5.2  | 8.0  | 6.5   | 28.2  | 112.5 | 15.2  | 45.1  | 63.9  | 9.8   | 26.3  | 32.5 | 0     |
| Wuhan        | 22.4 | 43.9 | 90.1  | 145.7 | 153.9 | 256.6 | 316.2 | 136.0 | 207.8 | 5.6   | 54.6 | 1.4   |
| Chongqing    | 9.3  | 29.0 | 3.4   | 114.8 | 126.6 | 241.6 | 81.1  | 62.6  | 194.5 | 91.0  | 56.8 | 16.2  |
| Beijing      | 3.0  | 3.4  | 10.7  | 5.5   | 23.6  | 91.0  | 235.6 | 118.6 | 71.1  | 16.4  | 0.2  | 0     |
| Urumqi       | 7.1  | 11.7 | 13.2  | 69.2  | 27.1  | 31.3  | 23.3  | 29.2  | 12.7  | 16.6  | 44.5 | 15.0  |
| Guangzhou    | 3.8  | 8.0  | 174.2 | 282.8 | 300.6 | 228.2 | 318.9 | 395.5 | 231.0 | 5.0   | 42.2 | 105.2 |

curve is smoother than the precipitation curve over this year, and there is little natural rainfall during the months of January, February, March, October, November, December with almost zero, but the production of the device is still significant. It means that even in those months when natural rainfall is low, the device can work effectively and there is still some water production.

In the case of Zhengzhou, the two curves look completely different, there is a strong peak of natural rainfall during the month of May, but the output curve of the device reaches the peak during the July, moreover, there still is some water production during the months of January, February, March, December, whereas the natural precipitation is low.

In addition, these results for the two cities are an objection to the view that this device is unfavorable in arid regions.

Fig. 6(e) and (f) shows the situations of Wuhan and Chongqing. In the first case, the main natural rainfall happens in the summer months, the period when the main water production by the device also occurs. During this period, there are two peaks shown in both curves. In the case of Chongqing, there is little rainfall during the months of January and March, even less than 10 mm per month. However, in the summer months, there are two maximum values shown in the precipitation curve. For the device output curve, it is smoother and the amount of water production doesn't change much over this year. Actually the peaks of the output curve and the precipitation curve are different in both cases. Except for June, there are still some similarities between the two curves.

Fig. 6(g) and (h) shows the natural precipitation and water production by this device in Beijing and Urumqi, respectively. In the first view, the two curves in both graphs are fairly similar.

In the case of Beijing, even the peak where the output curve reaches to the maximum value is the same with the precipitation curve. The output curve follows the precipitation curve in excellent correlation and is smoother.

When observing the case of Urumqi, we can see that there is a peak of natural rainfall during March and May, whereas there is little natural rainfall during the rest of the year. For the output curve, we can see that it's also smoother, the total values of water production distribute evenly over the year.

Fig. 6(i) represents the situation in Guangzhou, Guangdong. As we know, Guangzhou is located in the south of China, it's a coastal city where the summer is hot and winter is dry, thus the main portion of natural rainfall and water production by the device occurs during summer months. It can be seen that the two curves also are similar. However, from October to December, there seems to be a negative correlation between the two curves, what is worth mentioning, the average relative humidity during these months is comparatively low, because of this, the winter in Guangzhou is dry. Besides, there is still some positive correlation during the rest of the year.

In observing the graphs above, it is evident that they seem to support clearly the previously given argument with regard to the positive correlation between water production and natural



precipitation. However, there still exist some negative correlations that can't be neglected. We also notice that this negative correlation often appears in the dry season, in which the relative humidity is considerably lower. In Zhengzhou, the average relative humidity for 2013 is just 53%, we can see how the negative correlation is, as the output curve of the device is smoother, it shows that the water production does not rapidly increase or decrease, but slowly changes with time. There is still capacity for water production from the negative correlation even during periods of low natural precipitation.

We may conclude from this analysis that the arid season when little natural precipitation occurs is not necessarily unfavorable for this SCPP variant device, even in arid zones. When there is positive correlation, the principle of this device seems to be the same thannature, which also confirmed the feasibility of this engineering structure. And more importantly, this device is acting as an artificial stimulator of precipitation that is capable of increasing the water production during rainfalls.

4.2. Effectiveness

As a matter of fact, these few cases with the ideal data are not enough for thoroughly meaningful statistical results. From the positive correlation mentioned above, we aim at accurately characterize it thanks to the Pearson's correlation coefficient *r*, above nine stations calculated by:

$$r = \frac{\sum_{i=1}^{12} (x_i - \bar{x})(y_i - \bar{y})}{\sqrt{\sum_{i=1}^{12} (x_i - \bar{x})^2} \sqrt{\sum_{i=1}^{12} (y_i - \bar{y})^2}} \tag{16}$$

$$\bar{x} = \frac{1}{12} \sum_{i=1}^{12} x_i; \quad \bar{y} = \frac{1}{12} \sum_{i=1}^{12} y_i \tag{17}$$

where *x<sub>i</sub>* represents the monthly average value of water output; *y<sub>i</sub>* represents the monthly average value of natural precipitation;  $\bar{x}$  and  $\bar{y}$  are the mean of dataset.

Table 5 shows for the nine stations the annual natural precipitation totals and the correlation coefficient, respectively. As we can see, the maximum value of correlation coefficient is even up to 0.875, in Shijiazhuang, of which the natural precipitation is 508.3 mm for 2013. And for three other stations the correlation coefficients exceed 0.8. When the correlation coefficient is closer to 1 indicates a closed linear relationship between the two curves. It's strong correlation when the correlation coefficient is 0.6–1, and it is moderately related when the correlation coefficient is 0.4–0.6. That is to say, a highly correlated often appears between the two curves even in different stations. That also proved a close relation between the artificial precipitation inside a tube and the natural precipitation.

However, a careful reader may find that the units of water output are different from the units of natural precipitation, as the former are tons per month, while the latter are mm per month. Thus we need to choose an area over which the water output of the SCPP variant will be spread. In order to make the scatters much closer enable to compare, we take the density of water as  $1 \times 10^3$  kg/m<sup>3</sup>, and choose the total water are spread over an area of  $5 \times 10^6$  m<sup>2</sup> or 5 km<sup>2</sup>. Based on this, we can compare the annual means. Table 6 shows for the nine stations the annual natural precipitation, and water production by the device, both in tons. Take

the area for spreading mentioned above, we can get the water production in millimeters, and the ratio of the water production to natural precipitation.

Fig. 7 is the ratio-precipitation graph; by which we can get the efficiency of water production plotted versus the natural precipitation. It is obvious that the efficiency of water production is greater in those arid regions, such as Zhengzhou, Shijiazhuang and Urumqi. And it's less efficient in rainy regions such as Guangzhou. That is true, referring to Table 6, the natural precipitation of these situations as the denominator is different from each other, in contrast, the water production as the numerator is nearly the same order of magnitude. The distribution of those stations is distinguishable by natural precipitation, so that the arid cities and the rainy cities are located at both ends of the line, respectively. In addition, we can find an approximately linear distribution, which means that the efficiency is inversely proportional to the natural rainfall.

Moreover, when looking at the sunshine duration over the year, the arid regions such as Urumqi and Zhengzhou of which the annual natural precipitation are relatively low have abundant solar radiation. On the contrary, the cities located in wet regions have less sunshine time. There is no doubt that the temperature difference is a driving force of the convective motion, the greater this difference in temperature is, the stronger the natural air convection movement, thus more difficult for precipitation to occur as dilution of humid parcels occur. Meanwhile inside a tube, no dryer air comes to dilute the ascending air which is cooling inside the chimney and reaching the dew point. That means the device located in the dry region would be more effective to condense water than the natural phenomenon. As the natural precipitation includes many time-varying factors, to figure it out, maybe we need a lot of statistical data. But for now, we may at least come to a conclusion that this device is quite efficient and could increase the water production in arid regions.

The water production is given in millimeters if the water were spread over an area of  $5 \times 10^6$  m<sup>2</sup>.

Starr [29] studied a system that has a collection of tubes arranged in square shape with sides of 100 m and a mean air speed of 20 m per second. Assuming one gram of liquid water can be removed from each kilogram of air, the precipitation for the collecting area of several square kilometers would be nearly 30 cm.

Fig. 8 shows the humidity ratios of Urumqi in 2013. As we can calculate, the average humidity ratio of ambient air for this year was about 5.84 g/kg, and the average humidity ratio of condensed water by this device was about 2.3 g/kg. It means that we can extract nearly 2.3 g of liquid water from each kilogram of air even in those arid regions such as in Urumqi, or we can get water of approximately 70 cm high if the water is formed in this 100 m square tube and spread over the same area. Actually, we calculated that the water output by this device which is a circular cylinder with a diameter of 100 m in Urumqi would be nearly 163.6 cm if the total water is spread over an area of  $5 \times 10^6$  m<sup>2</sup>. Obviously, this amount is considerable.

What's more, from Fig. 8 we also find that there are some months whose average humidity ratio of water production is close to the environmental humidity ratio. Due to the small collector (black tubes) that help to assume that the temperature of hot air at the entrance is 5 K higher than that of the environment keeping the same humidity than ambient thanks to hot water showers, it is

**Table 5**  
Annual Natural precipitation for 2013 and correlation coefficient at nine stations.

|                         | Chengdu | Shanghai | Shijiazhuang | Zhengzhou | Wuhan  | Chongqing | Beijing | Urumqi | Guangzhou |
|-------------------------|---------|----------|--------------|-----------|--------|-----------|---------|--------|-----------|
| NP, mm                  | 1343.3  | 1173.4   | 508.3        | 353.2     | 1434.2 | 1026.9    | 579.1   | 300.9  | 2095.4    |
| Correlation coefficient | 0.816   | 0.598    | 0.875        | 0.455     | 0.778  | 0.578     | 0.862   | 0.542  | 0.827     |

**Table 6**  
Annual natural precipitation (NP), water production (WP) by SCPP and sunshine duration for 2013 at nine stations.

|              | NP (mm) | WP (10 <sup>6</sup> t) | WP (mm) | Ratio (WP/NP) | Sunshine duration (h) |
|--------------|---------|------------------------|---------|---------------|-----------------------|
| Chengdu      | 1343.3  | 29.71                  | 5942    | 4.42          | 1128.8                |
| Shanghai     | 1173.4  | 23.62                  | 4724    | 4.03          | 1864.7                |
| Shijiazhuang | 508.3   | 17.08                  | 3416    | 6.72          | 1716.8                |
| Zhengzhou    | 353.2   | 12.87                  | 2574    | 7.29          | 1925.6                |
| Wuhan        | 1434.2  | 29.37                  | 5874    | 4.10          | 2092.5                |
| Chongqing    | 1026.9  | 27.40                  | 5480    | 5.34          | 1213.7                |
| Beijing      | 579.1   | 14.59                  | 2918    | 5.04          | 2371.1                |
| Urumqi       | 300.9   | 8.18                   | 1636    | 5.44          | 3068.6                |
| Guangzhou    | 2095.4  | 37.92                  | 7584    | 3.62          | 1582.9                |

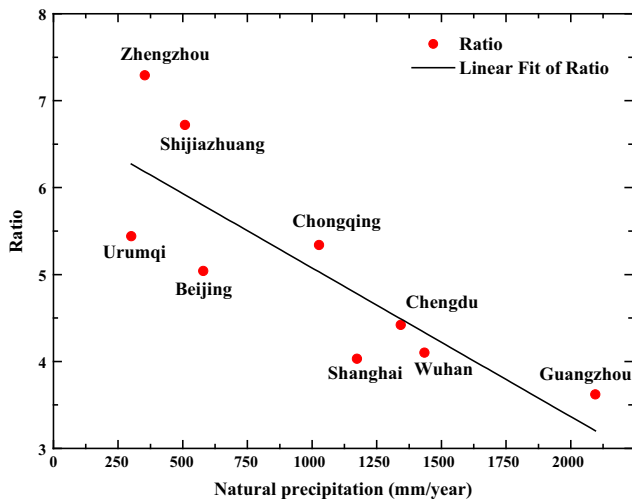


**Fig. 7.** Efficiency of the SCPP variant device (ratio of water production distributed over an area  $5 \times 10^6 \text{ m}^2$  to natural precipitation) is shown versus the precipitation.

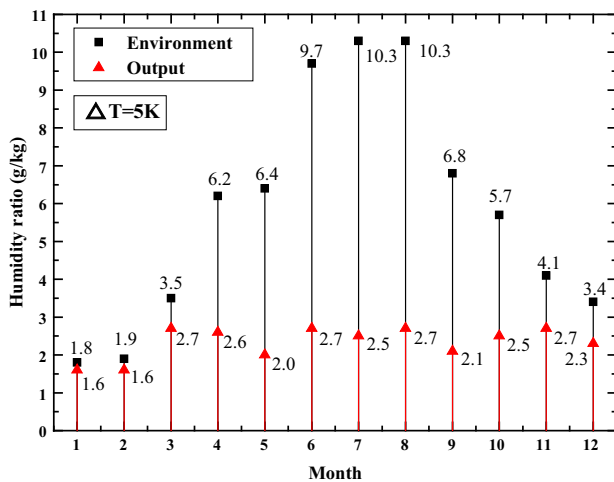


**Fig. 8.** Average humidity ratios of ambient air and water production for 2013 in Urumqi.

no doubt that a higher temperature increase of the water at the collector would lead to higher RH% level at the entrance and more water production by the SCPP variant, as does the humidity ratio. If the inlet temperature of hot air is higher, the humidity ratio of water production would rise to reach even exceed the humidity ratio of environment. In other words, there are still large rise space during the months of this year in Urumqi, thus we believe that there is still capacity for this device under favorable conditions

to produce considerable amounts of water. As shown in Fig. 9, the water production increases with the increasing inlet temperature and relative humidity. The initial conditions include air temperature at the entrance of the chimney and relative humidity are average values of Urumqi for the calendar year 2013. Referring to Table 5, the sunshine duration of Urumqi is the most important of the 9 cities considered so the temperature difference in there is relatively high, and accordingly, able to produce more water. Under certain economic conditions, we can also raise the temperature and relative humidity of hot air as much as possible at the entrance of chimney to obtain more water production (see Table 7).

Compared with the natural rainfall, the water production by SCPP variant seems to be important in spite of several assumptions made for our calculations.

In China, with the rapid growth of industrialization and urbanization, most cities, especially mega-cities, are having a huge demand for water. Though the domestic water is becoming scarce, we are encouraged by the SCPP variant presented in this article because of the huge potential for water supply. As shown in Table 6, water production by the SCPP variant is almost equal to domestic water needed for 2013 in Beijing and Shanghai. In Chongqing, the amount of water production by SCPP exceeds the domestic water use for this year. In the ideal situation, the application of SCPP variant for water production is very effective. Moreover, we found that the water supply by the SCPP variant can benefit several millions of people.

4.3. Environmental effects

Although there is a great potential for extracting water from air by the SCPP variant, the water resource in the atmospheric strata seems to be easily exhausted by this process. Thus maybe this process causes some problems?

What are the effect on the atmospheric circulation or the local climate? Could it have the damaging effect of reducing natural rainfall? To answer these questions, we may notice another artificial process that could cause a similar effect: irrigation, which started some thousands of years ago. DeAngelis [35] found that in the USA there was some increase in precipitation of 15–30% during July from the eastern most part of the aquifer to as far downwind as Indiana. Lo and Famiglietti [36] identified that irrigation in California’s Central Valley initiates an anthropogenic loop in the regional hydrological cycle, in which summer precipitation is increased by 15%. Irrigation would increase evapotranspiration

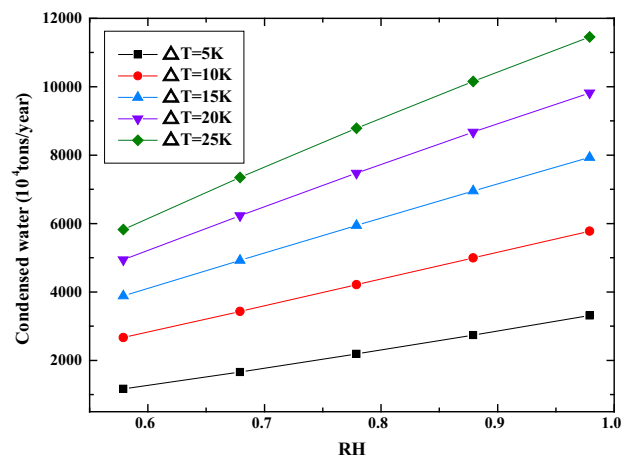


**Fig. 9.** Condensed water versus RH for different temperature differences at the entrance.

**Table 7**  
Water-use efficiency of SCPP for 2013 in several cities.

|           | Domestic water, billion cubic meters | Water use per capita (m <sup>3</sup> /person) | Water production by SCPP variant (10 <sup>9</sup> m <sup>3</sup> /year) | Water supply by SCPP variant by population, inhabitants |
|-----------|--------------------------------------|---|---|---|
| Beijing   | 1.63                                 | 173.9   | 1.459   | 8389880   |
| Shanghai  | 2.57                                 | 513.9   | 2.362   | 4596225   |
| Chongqing | 1.81                                 | 283.7   | 2.740   | 9658090   |

thus affecting convection; the resulting increase in water vapor export impacts the atmospheric circulation. Significant increases in precipitation occurs in irrigated areas [37]. Meanwhile, it seems evident that the contribution of downwind precipitation is greater when the evapotranspiration is higher. Since the height of this SCPP device is great enough, the adiabatically ascending air parcel within the chimney should presently reach the lifting condensation level similar to cloud formation, and then the further lifting within the chimney will be pseudo adiabatic, removing liquid water from the rising air and liberating the latent heat. In the effects of the initial ejecting momentum, the buoyancy effect, considerable amounts of cloud material would be rejected at the exhaust end in the form of a plume. Atmospheric circulation and rainfall are formed. Under favorable conditions, thunderstorms might be spawned and drift away. Zhou et al. [38] found that the SCPP increases the chance of rainfalls especially for low-humidity air in the desert region that is sunny but the humidity of air is low. The use of SCPP variants over the warm ocean waters along the coast can also be used for seawater desalination, with increasing the rainfalls and enhancing the regional water cycle. There are also some possible uses of the device, such as air removal for pollution control and heat removal from the lower atmosphere to higher elevations [29].

However, the actual construction of this device is a matter that poses problems of expense and engineering feasibility. To reduce its geometry sizes such as height and diameter, we could take a series of optimization measures. For example, we could furnish moist to the intake air with high relative humidity that is near saturation, thus reduced the condensation level and the chimney height. Meanwhile, a small feasible experimental structure further can be constructed to be favorable for feasible operating conditions from the scientific point of view. It is possible that further research will find solutions to these problems, exploiting useful applications in other areas.

For example, we could furnish much moister to the intake air with high relative humidity that is near saturation: the results will thus be to reduce the condensation level and the chimney height needed. Meanwhile, a small feasible experimental structure further can be constructed to be favorable for feasible operating conditions from the scientific point of view.

#### 4.4. Collector cost reduction

In the traditional solar chimney, the expense of the collector canopy (glass or plastics) occupies a large amount of the total investment [20]. If the canopy is replaced by black tubes, the total price will go down. We assume that the cost of plastic polyethylene tubing  $\varnothing 100$  mm (5.3 mm in thickness, 0.8 MPa pressure) is about 17 ¥ per meter (about 2.4 €/m or US\$ 2.6/m) in China. Adding 500 km of this tubing will cost 8.5 million ¥. If done in 10 sections of 50 km each, tube connections and pumps plus water showers at the entrance of the chimney (used to keep the humidity identical to ambient, but with the air temperature 5 °C higher) will cost about 2 125 000 ¥. The tubing is spaced as in Fig. 3 over an area of 5 km<sup>2</sup> and under the tubing and space in between, the ground

is painted dark (or asphalted) in order to store thermal energy underground. The solar insolation in China is about 4200–6700 MJ/(m<sup>2</sup> a), and a 5 km<sup>2</sup> collector area receive enough energy to warm the amount of moist air needed. Earthworks and engineering cost about 10.6 million ¥. Total 21 million ¥ to be compared to the collector cost estimated by Kraetzig [7] to be nearly 3.5–4.6 billion ¥.

## 5. Discussion

In this work, we set the temperature of the black tubes to be sufficiently higher than the ambient air to warm the air entering the chimney by about 5 K higher than ambient. Actually, it is not necessary to increase the air temperature difference with ambient to be too high. The temperature of the black tubes is hot enough to warm the air that enters the chimney to about 5 K higher than the ambient air on a 24 h basis (thermal storage for night operation). This means the tubes and the ground below are warmer than 5 K. Also the temperature of the water inside the black tubes is enough to provide sufficiently hot water (which can be sea water or brackish water) to keep the humidity at the same level than ambient as it was naturally outside. This means that if the RH = 60% and ambient is 25 °C, thus at chimney entrance air temperature is 30 °C and RH% = 60% but the hotter air contains about 8 more grams of water per m<sup>3</sup> of air.

Also if the temperature of the air that enters the chimney is 20 K higher than ambient, the condensation level will be much higher and that less water or even no water at all will be produced, and it will cost more in black tubing. This can be good if we want to produce electricity for a traditional SCPP equipped with turbines. On the other side, if we want to produce more water, we can only warm the air entering under the tower of only 1 or 2 K in order to have a lower condensation level, but the initial speed of the airflow will be smaller (until the condensation inside starts and the latent heat released inside the chimney warms the inner air, which then sucks all the air column during its ascension). In this latter case, the risk is that at the warmer hours of the day, if there is little condensation inside the tower, the air speed will stay small.

## 6. Conclusions

A mathematic model has been developed for a one-dimensional compressible flow and heat transfer in a SCPP variant. The effectiveness of this engineering structure is analyzed in comparison to natural precipitation at nine cities in China. The following conclusions can be drawn from the analyses.

- The arid seasons or arid regions in which little natural precipitation occurs is not necessarily unfavorable for this SCPP variant, especially as it is able to increase the water production. The efficiency of this engineering structure is inversely proportional to the natural rainfall.
- Under favorable conditions, the amount of water production by this SCPP variant is considerable. The water supply by the SCPP variant of the population can possibly benefit several millions of people.
- Since the height of this device is great enough, atmospheric circulation and rainfall are formed. Under favorable conditions, thunderstorms might be spawned and drift away.

## Author contributions

T.M. and T.G. contributed equally to the work. R.K.R. and T.M. raised the idea, R.K.R., T.M., W.L. and A.K. discussed the idea and considered the methodology, T.G. performed the simulation, T.G.

and T.M. and drafted the manuscript, all the authors revised whole manuscript, W.L. and A.K. read through the whole manuscript and raised some suggestions, R.K.R. polished the whole manuscript.

### Acknowledgements

This research was supported in part by Scientific Research Foundation of Wuhan University of Technology (No. 40120237), in part by Fundamental Research Funds for the Central Universities (WUT Grant No. 2016IVA029), and in part by the National Natural Science Foundation of China (No. 51576077 and No. 51106060). The authors would also like to express their gratitude to the 3 anonymous reviewers for their comments and questions which helped to significantly improve the article.

### References

- [1] Addams L, Boccaletti G, Kerlin M, Stuchtey M. Charting our water future: economic frameworks to inform decision-making. New York: McKinsey & Company; 2009.
- [2] Ming T, de\_Richter R, Liu W, Caillol S. Fighting global warming by climate engineering: Is the Earth radiation management and the solar radiation management any option for fighting climate change? *Renew Sustain Energy Rev* 2014;31:792–834.
- [3] Zhou X, Wang F, Ochieng RM. A review of solar chimney power technology. *Renew Sustain Energy Rev* 2010;14:2315–38.
- [4] Haaf W. Solar tower, Part II: Preliminary test results from the Manzanares pilot plant. *Int J Sol Energy* 1984;2:41–61.
- [5] Koonsrisuk A. Comparison of conventional solar chimney power plants and sloped solar chimney power plants using second law analysis. *Sol Energy* 2013;98:78–84.
- [6] Koonsrisuk A, Chitsomboon T. A single dimensionless variable for solar chimney power plant modeling. *Sol Energy* 2009;83:2136–43.
- [7] Kraetzig WB. Physics, computer simulation and optimization of thermo-fluidmechanical processes of solar updraft power plants. *Sol Energy* 2013;98:2–11.
- [8] Bernardes MADS, Backström TWV. Evaluation of operational control strategies applicable to solar chimney power plants. *Sol Energy* 2010;84:277–88.
- [9] Pretorius JP, Kroger DG. Solar chimney power plant performance. *J Sol Energy – Trans ASME* 2006;128:302–11.
- [10] Fasel HF, Meng F, Shams E, Gross A. CFD analysis for solar chimney power plants. *Sol Energy* 2013;98:12–22.
- [11] Ming T, Gui J, Richter R, Pan Y, Xu G. Numerical analysis on the solar updraft power plant system with a blockage. *Sol Energy* 2013;98:58–69.
- [12] Ferreira AG, Maia CB, Cortez MFB, Valle RM. Technical feasibility assessment of a solar chimney for food drying. *Sol Energy* 2008;82:198–205.
- [13] Maia CB, Ferreira AG, Valle RM, Cortez MFB. Theoretical evaluation of the influence of geometric parameters and materials on the behavior of the airflow in a solar chimney. *Comput Fluids* 2009;38:625–36.
- [14] Maia CB, Castro Silva JO, Cabezas-Gómez L, Hanriot SM, Ferreira AG. Energy and exergy analysis of the airflow inside a solar chimney. *Renew Sustain Energy Rev* 2013;27:350–61.
- [15] Patel SK, Prasad D, Ahmed MR. Computational studies on the effect of geometric parameters on the performance of a solar chimney power plant. *Energy Convers Manage* 2014;77:424–31.
- [16] Fei C, Liang Z, Guo L. Simulation of a sloped solar chimney power plant in Lanzhou. *Energy Convers Manage* 2011;52:2360–6.
- [17] Ninic N, Nizetic S. Elementary theory of stationary vortex columns for solar chimney power plants. *Sol Energy* 2009;83:462–76.
- [18] Nizetic S, Ninic N, Klarin B. Analysis and feasibility of implementing solar chimney power plants in the Mediterranean region. *Energy* 2008;33:1680–90.
- [19] Nizetic S, Klarin B. A simplified analytical approach for evaluation of the optimal ratio of pressure drop across the turbine in solar chimney power plants. *Appl Energy* 2010;87:587–91.
- [20] Pasumarthi N, Sherif SA. Experimental and theoretical performance of a demonstration solar chimney model – Part II: Experimental and theoretical results and economic analysis. *Int J Energy Res* 1998;22:443–61.
- [21] Schlaich J, Bergermann R, Schiel W, Weinrebe G. Design of commercial solar updraft tower systems—utilization of solar induced convective flows for power generation. *J SolEnergy Eng* 2005;127:117–24.
- [22] Zheng Z, He S. Modeling and characteristics analysis of hybrid cooling-tower-solar-chimney system. *Energy Convers Manage* 2015;95:59–68.
- [23] Kashiwa B, Kashiwa CB. The solar cyclone: a solar chimney for harvesting atmospheric water. *Energy* 2008;33:331–9.
- [24] Mourtada A, Arkahdan AN, Karout YM. Solar chimney electricity from the sun. In: 2012 international conference on renewable energies for developing countries (REDEC); 2012.
- [25] Bonnelle D. Solar chimney, water spraying energy tower, and linked renewable energy conversion devices: presentation, criticism and proposals. PhD, University Claude Bernard-Lyon; 2004.
- [26] Papageorgiou CD. Floating solar chimney technology. Available: <<http://vortexengine.ca/Links/Floating.pdf>>.
- [27] Zhou X, Xiao B, Liu W, Guo X, Yang J, Fan J. Comparison of classical solar chimney power system and combined solar chimney system for power generation and seawater desalination. *Desalination* 2010;250:249–56.
- [28] Starr VP, Anati DA, Gaut NE. Controlled atmospheric convection in an engineered structure. *Nord Hydrol* 1972;3:1–21.
- [29] Starr VP, Anati DA. Experimental engineering procedure for the recovery of liquid water from the atmospheric vapor content. *Pure Appl Geophys* 1971;86:205–8.
- [30] Carte AE. Mine shafts as a cloud physics facility. In: *Proc int conf on cloud phys*; 1968. p. 384–8.
- [31] Lambrechts JDV. The value of water drainage in upcast mine shafts and fan drifts. *J Chem Met Min Soc SA* 1956:307–24.
- [32] Starr VP, Anati D, Salstein D. Effectiveness of controlled convection in producing precipitation. *J Geophys Res* 1974;79:4047–52.
- [33] Bernardes MAD, Voss A, Weinrebe G. Thermal and technical analyses of solar chimneys. *Sol Energy* 2003;75:511–24.
- [34] von Backström TW, Gannon AJ. Compressible flow through solar power plant chimneys. *J SolEnergy Eng* 2000;122:138–45.
- [35] DeAngelis A, Dominguez F, Fan Y, Robock A, Kustu MD, Robinson D. Evidence of enhanced precipitation due to irrigation over the Great Plains of the United States. *J Geophys Res: Atmos* (1984–2012) 2010;115.
- [36] Lo MH, Famiglietti JS. Irrigation in California's Central Valley strengthens the southwestern US water cycle. *Geophys Res Lett* 2013;40:301–6.
- [37] Puma M, Cook B. Effects of irrigation on global climate during the 20th century. *J Geophys Res: Atmos* (1984–2012) 2010;115.
- [38] Zhou X, Yang J, Xiao B, Shi X. Special climate around a commercial solar chimney power plant. *J Energy Eng* 2008;134:6–14.